Article

The Electronic Role of DNA-Functionalized Carbon Nanotubes: Efficacy for in Situ Polymerization of Conducting Polymer Nanocomposites

Yufeng Ma, Pui Lam Chiu, Arnaldo Serrano, Shah R. Ali, Alex M. Chen, and Huixin He

J. Am. Chem. Soc., **2008**, 130 (25), 7921-7928 • DOI: 10.1021/ja7112189 • Publication Date (Web): 03 June 2008

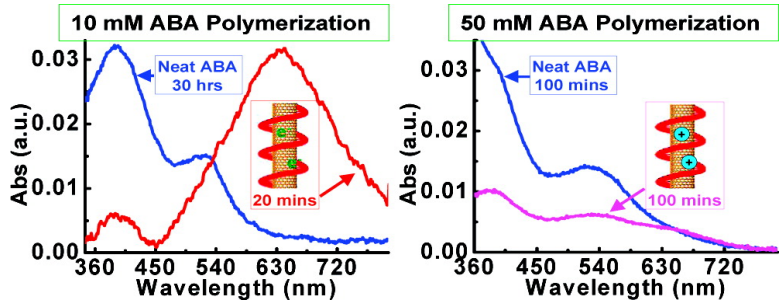

More About This Article

Additional resources and features associated with this article are available within the HTML version:

- Supporting Information
- Access to high resolution figures
- Links to articles and content related to this article
- Copyright permission to reproduce figures and/or text from this article

View the Full Text HTML

J|A|C|S
ARTICLES

Published on Web 06/03/2008

The Electronic Role of DNA-Functionalized Carbon Nanotubes: Efficacy for in Situ Polymerization of Conducting Polymer Nanocomposites

Yufeng Ma, Pui Lam Chiu, Arnaldo Serrano, Shah R. Ali, Alex M. Chen, and Huixin He*

Chemistry Department, Rutgers University, Newark, New Jersey 07102

Received December 18, 2007; E-mail: huixinhe@newark.rutgers.edu

Abstract: We have found that the polymerization process was 4,500 times faster when a self-doped polyaniline nanocomposite was fabricated using in situ polymerization in the presence of single-stranded DNA-dispersed and -functionalized single-walled carbon nanotubes (ssDNA−SWNTs). More importantly, the quality of the composite was significantly improved: fewer short oligomers were produced, and the self-doped polyaniline backbone had a longer conjugation length and existed in the more stable and conductive emeraldine state. The functionality of the boronic acid group in the composite and the highly improved electronic performance may lead to broad applications of the composite in flexible electronic devices. Blending of preformed polymer with carbon nanotubes is straightforward and widely used to fabricate nanocomposites. We demonstrate that this simple mixing approach might not fully and synergistically combine the merits of each individual component. Surprisingly, these advantages also cannot be obtained using in situ polymerization with preoxidized ssDNA−SWNTs, which is renowned as the "seed" method for production of conducting-polymer nanowires. The electronic structures of the carbon nanotubes and the monomer−nanotube interaction during polymerization greatly impact the kinetics of nanocomposite fabrication and the electronic performance of the resulting composites.

Introduction

Inspired by the remarkable electrical and thermal conductivities and superior mechanical properties of carbon nanotubes (CNTs), researchers have invested tremendous effort over the past decade in preparing composites of polymers and carbon nanotubes, aiming to synergistically combine the merits of each individual component.[1–9] Enhancement of the nanocomposites is critically dependent on monomer−nanotube interfacial interactions during polymerization and polymer−nanotube interfacial interactions after polymerization. Intense research efforts have been devoted to studying the effect of the polymer−nanotube interactions on the enhancement of the composites.[5,10,11] However, the impacts of the electronic structure of the CNTs and the monomer−nanotube interfacial interactions on the kinetics of nanocomposite fabrication and the quality of the obtained composite have yet to be addressed. The objective of the present work was to study these effects.

The catalytic behavior of CNTs has been intensely debated. For a long time it was believed that the electrooxidative catalytic properties of CNTs could be exploited in a wide variety of applications, including chemical sensors and biosensors. Recently, Compton and co-workers[12,13] demonstrated that the previously reported electrocatalytic behavior of CNTs may in fact arise from iron oxide residues rather than from any intrinsic properties of the nanotubes. These residues are left behind during the fabrication process and are difficult to completely remove even with acid pretreatment. On the other hand, the catalytic capability of CNTs was recently demonstrated[14] in the reduction of some organic receptors and inorganic molecules by water. Zheng and co-workers[15] demonstrated that single-stranded DNA-functionalized single-walled carbon nanotubes (ssDNA−SWNTs) facilitated photoinduced reduction of Ag^+.

(1) Tasis, D.; Tagmatarchis, N.; Bianco, A.; Prato, M. *Chem. Rev.* **2006**, *106*, 1105–1136.
(2) Iijima, S. *Nature* **1991**, *354*, 56–58.
(3) Ajayan, P. M.; Stephan, O.; Colliex, C.; Trauth, D. *Science* **1994**, *265*, 1212–1214.
(4) Dai, L.; Mau, A. W. H. *Adv. Mater.* **2001**, *13*, 899–913.
(5) Zengin, H.; Zhou, W.; Jin, J.; Czerw, R.; Smith, J. D. W.; Echegoyen, L.; Carroll, D. L.; Foulger, S. H.; Ballato, J. *Adv. Mater.* **2002**, *14*, 1480–1483.
(6) Cochet, M.; Maser, W. K.; Benito, A. M.; Callejas, M. A.; Martínez, M. T.; Benoit, J.-M.; Schreiber, J.; Chauvet, O. *Chem. Commun.* **2001**, 1450.
(7) Sainz, R.; Benito, A. M.; Martínez, M. T.; Galindo, J. F.; Sotres, J.; Baró, A. M.; Corraze, B.; Chauvet, O.; Maser, W. K. *Adv. Mater.* **2005**, *17*, 278–281.
(8) Moniruzzaman, M.; Winey, K. I. *Macromolecules* **2006**, *39*, 5194–5205.
(9) Grossiord, N.; Loos, J.; Regev, O.; Koning, C. E. *Chem. Mater.* **2006**, *18*, 1089–1099.
(10) Moniruzzaman, M.; Chattopadhyay, J.; Billups, W. E.; Winey, K. I. *Nano Lett.* **2007**, *7*, 1178–1185.
(11) Schadler, L. S.; Kumar, S. K.; Benicewicz, B. C.; Lewis, S. L.; Harton, S. E. *MRS Bull.* **2007**, *32*, 335–340.
(12) Sljukic, B.; Banks, C. E.; Compton, R. G. *Nano Lett.* **2006**, *6*, 1556–1558.
(13) Banks, C. E.; Crossley, A.; Salter, C.; Wilkins, S. J.; Compton, R. G. *Angew. Chem., Int. Ed.* **2006**, *45*, 2533–2537.
(14) O'Connell, M. J.; Eibergen, E. E.; Doorn, S. K. *Nat. Mater.* **2005**, *4*, 412–418.
(15) Zheng, M.; Rostovtsev, V. V. *J. Am. Chem. Soc.* **2006**, *128*, 7702–7703.

In this work, we have found that ssDNA−SWNTs are highly effective in promoting in situ fabrication of a self-doped polyaniline nanocomposite by oxidative polymerization. We have demonstrated that the observed "catalytic" effect of the ssDNA−SWNTs is due to preconcentration of monomers along the ssDNA−SWNTs and electronic interactions between the monomers and ssDNA−SWNTs rather than to catalyst residues (iron oxide particles) present in the ssDNA−SWNTs. The catalytic efficacy was strongly dependent on the electronic structure of the CNTs. The polymerization rate was dramatically decreased in the presence of preoxidized ssDNA−SWNTs, and the electronic and molecular structures of the poly(aniline boronic acid) (PABA) in the resulting composite were very different from those of the PABA in composites fabricated using intact ssDNA−SWNTs. The fabrication process significantly impacted the performance of the nanocomposite obtained.

There is an increasing enthusiasm for the use of SWNT networks as conductive flexible electrodes in a wide variety of applications.[16–22] However, all of the reported conductivities of the SWNT networks were significantly lower than that of a SWNT rope (axial conductivity).[23] We have found that the conductivity of the network can be greatly improved by in situ polymerization of a thin layer of conductive self-doped polyaniline on the carbon nanotubes.[24] However these advantages cannot be obtained by simple mixing of the preformed polymer with the ssDNA−SWNTs. We have also found that these advantages cannot be obtained using the "seed" approach, in which monomers are polymerized in situ in the presence of preoxidized ssDNA−SWNTs, even though this approach has been reported to efficiently produce conducting-polymer nanowires.[25,26]

Experimental Section

Materials. 3-Aminophenylboronic acid hemisulfate salt (ABA), potassium fluoride, and all other chemicals were purchased from Aldrich and used as received. Single-stranded DNA with sequence $d(T)_{30}$ was purchased from Integrated DNA Technologies. All of the solutions were prepared using deionized water (18.2 MΩ) (Nanopore water, Barnstead).

Dispersion of SWNTs into Water Solution. HiPco Purified SWNTs were purchased from Carbon Nanotechnologies and dispersed into water using the method described by Zheng et al.[27] As a result, a highly dispersed and ssDNA-functionalized SWNT solution was obtained. To remove free ssDNA from the dispersed solution, the solution was dialyzed with a Microcon YM-100 centrifugal filter unit (Millipore) for 4 h. The electronic structure of the ssDNA−SWNTs was studied using a Cary 500 UV−vis−near-infrared (NIR) spectrophotometer in double-beam mode.

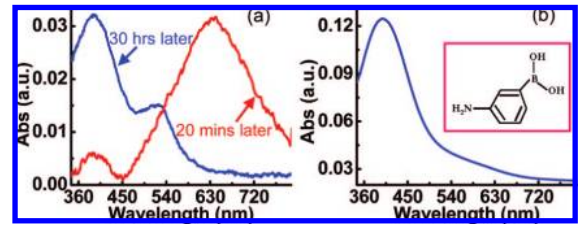

Figure 1. (a) UV−vis−NIR spectra after polymerization of 10 mM ABA in 0.5 M H_2SO_4 at 16 °C for (blue curve) 30 h in the absence of and (red curve) 20 min in the presence of ssDNA−SWNTs (SWNT/ABA ratio = 1:200). (b) UV−vis−NIR spectrum of the oligomer solution obtained after removal of the PABA from a neat polymer solution obtained using the same polymerization conditions as the blue curve in (a) except that the concentration of ABA was 50 mM. The inset shows the chemical structure of ABA.

In Situ Monitoring of ABA Polymerization. To study the catalytic effect of ssDNA−SWNTs, we used UV−vis−NIR absorption spectroscopy to monitor the polymerization processes in situ in the presence or absence of ssDNA−SWNTs. ABA monomer (2.5 or 10 mM) and KF (40 mM) were dissolved in 0.5 M H_2SO_4, and then 91.4 μL of ssDNA−SWNTs was added to 2.5 mL of the prepared monomer solution. The mixture was bubbled with nitrogen for 30 min, after which the polymerization was initiated by adding 0.5 mL of 37.5 mM $(NH_4)_2S_2O_8$ (APS) in 0.5 M H_2SO_4 dropwise to the mixture. All of the experiments were performed at 16 °C to avoid condensation of water on the cuvette. Control experiments were performed under the same conditions without ssDNA−SWNTs. Because the polymerization rate was smaller in the absence of ssDNA−SWNTs, another control experiment with a higher concentration of ABA (50 mM) was also performed. All of the spectra were obtained using a Cary 500 UV−vis−NIR spectrophotometer in double-beam mode.

Results and Discussion

Polymerization of ABA without ssDNA−SWNTs. Becaue of its highly conjugated polyaniline backbone, PABA exhibits different electronic properties than the ABA monomers. Therefore, the formation of PABA by oxidative polymerization of ABA can be monitored using UV−vis−NIR electronic absorption spectroscopy.

Figure 1a shows the UV−vis−NIR spectrum (blue curve) after 30 h of polymerization of 10 mM ABA in the absence of ssDNA−SWNTs. The spectrum shows two broad peaks at 390 and 530 nm. The peak at 530 nm was assigned to the excitation of the quinone diimine structure (−N═Q═N−) in the polyaniline backbone. The position of this peak depends on the conjugation length and the oxidation state of the polyaniline backbone.[28] The λ_{max} value of the 530 nm peak was much less than that for PABA polymerized at 0 °C.[29] This blue shift is consistent with previous reports that polymerization at higher temperatures produces polymers with shorter conjugation lengths

(16) Saran, N.; Parikh, K.; Suh, S.-S.; Muñoz, E.; Kolla, H.; Manohar, S. K. *J. Am. Chem. Soc.* **2004**, *126*, 4462–4463.
(17) Star, A.; Tu, E.; Niemann, J.; Galbriel, J.-C. P.; Joiner, C. S.; Valcke, C. *Proc. Natl. Acad. Sci. U.S.A.* **2006**, *103*, 921–926.
(18) Hur, S.-H.; Yoon, M.-H.; Gaur, A.; Shim, M.; Facchetti, A.; Marks, T. J.; Rogers, J. A. *J. Am. Chem. Soc.* **2005**, *127*, 13808–13809.
(19) Pasquier, A. D.; Unalan, H. E.; Kanwal, A.; Miller, A. D.; Chhowalla, M. *Appl. Phys. Lett.* **2005**, *87*, 203511.
(20) Wu, Z.; Chen, Z.; Du, X.; Logan, J. M.; Sippel, J.; Nikolou, M.; Kamaras, K.; Reynolds, J. R.; Tanner, D. B.; Hebard, A. F.; Rinzler, A. G. *Science* **2004**, *305*, 1273–1276.
(21) Artukovic, E.; Kaempgen, M.; Hecht, D. S.; Roth, S.; Grünera, G. *Nano Lett.* **2005**, *5*, 757–760.
(22) Li, J.; Hu, L.; Wang, L.; Zhou, Y.; Gruner, G.; Marks, T. J. *Nano Lett.* **2006**, *6*, 2472–2477.
(23) Thess, A.; Lee, R.; Nikolaev, P.; Dai, H. J.; Petit, P.; Robert, J.; Xu, C. H.; Lee, Y. H.; Kim, S. G.; Rinzler, A. G.; Colbert, D. T.; Scuseria, G. E.; Tomanek, D.; Fischer, J. E.; Smalley, R. E. *Science* **1996**, *273*, 483–487.
(24) Ma, Y. F.; Cheung, W.; Wei, D. G.; Bogozi, A.; Chiu, P. L.; Wang, L.; Pontoriero, F.; Mendelsohn, R.; He, H. X. *ACS Nano*, submitted for publication, 2008.
(25) Zhang, X.; Manohar, S. K. *J. Am. Chem. Soc.* **2004**, *126*, 12714–12715.
(26) Zhang, X. Y.; Goux, W. J.; Manohar, S. K. *J. Am. Chem. Soc.* **2004**, *126*, 4502–4503.
(27) Zheng, M.; Jagota, A.; Semke, E. D.; Diner, B. A.; Mclean, R. S.; Lustig, S. R.; Richardson, R. E.; Tassi, N. G. *Nat. Mater.* **2003**, *2*, 338–342.
(28) Stilwell, D. S.; Park, S.-M. *J. Electrochem. Soc.* **1989**, *136*, 427–433.
(29) Ma, Y. F.; Ali, S. R.; Wang, L.; Chiu, P. L.; Mendelsohn, R.; He, H. X. *J. Am. Chem. Soc.* **2006**, *128*, 12064–12065.

and more-branched structures.[14,15] The absorption peak at 390 nm has previously been assigned to the localized polaron band when the polyaniline backbone existed in the lower oxidation state of emeraldine[28,30] or to the quinone diimine structure in low-molecular-weight aniline oligomers.[31] Through centrifugation of the obtained polymer solution, a yellowish supernatant showing a strong UV absorption peak at 390 nm (Figure 1b) was obtained. Therefore, we conclude that both short ABA oligomers and PABA polymers were produced in this polymerization process.

Polymerization of ABA with ssDNA−SWNTs. When the polymerization was performed in the presence of a small amount of ssDNA−SWNTs, the UV−vis−NIR spectrum (red curve in Figure 1a) also showed two broad bands but was very different from the previous spectrum. The control UV−vis−NIR spectroscopic study was performed with the same concentration of ssDNA−SWNTs, showing that the absorption was dominated by the polymer, with little contribution from the nanotubes other than modifying the absorption spectrum of the polymer.

First of all, the absorption peak for the excitation of the quinone diimine structure was much broader and greatly red-shifted, from a λ_{max} of 530 nm in the neat polymer (Figure 1a, blue curve) to 622 nm in the composite (Figure 1a, red curve). One possible explanation for this red shift is that the PABA produced in the presence of ssDNA−SWNTs had a longer conjugation length and existed more in the stable and conductive emeraldine state, as proposed in our previous work.[29]

Second, the intensity of the peak was much greater than that of the polymerization without nanotubes. Without ssDNA−SWNTs in the solution, we were unable to detect any polymer formation after 20 min of polymerization. In the presence of ssDNA−SWNTs, however, the PABA peak intensity after 20 min is similar to that for the peak after 30 h polymerization of ABA without ssDNA−SWNTs. If it is assumed that the molar absorption extinction coefficient of the PABA is constant,[19] then the absorbance reflects the concentration of PABA formed in the reaction mixture. This result suggests that the polymerization efficiency was significantly increased by addition of ssDNA−SWNTs to the polymerization solution.

Finally, the intensity of the ABA oligomer peak at 390 nm was much smaller than that of the peak for the quinoid exciton transition of the PABA polymer, in contrast to the situation for polymerization without SWNTs. This result indicates that ssDNA−SWNTs largely eliminate the formation of ABA oligomers, as discussed in greater detail in the following section.

In Situ Study of the Polymerization Process Using UV−vis−NIR Spectroscopy. Figure 2a shows the evolution of UV−vis−NIR spectra recorded at various time intervals during the course of polymerization of 10 mM ABA in the presence of 0.5 wt % ssDNA−SWNTs (this concentration of nanotubes was chosen on the basis of recent reports that 0.5 wt % CNTs could reach electronic percolation[32]). In this polymerization mixture, the ratio of ssDNA−SWNTs to ABA by weight (hereafter called the SWNT/ABA ratio) was 1:200. The intensities of the peaks increased with polymerization time (Figure 2b). The peak at 622 nm grew more rapidly in the beginning and more slowly at later times. This behavior differed from that for the neat ABA polymerization, where the intensity at 530 nm increased at a much lower but constant rate over the

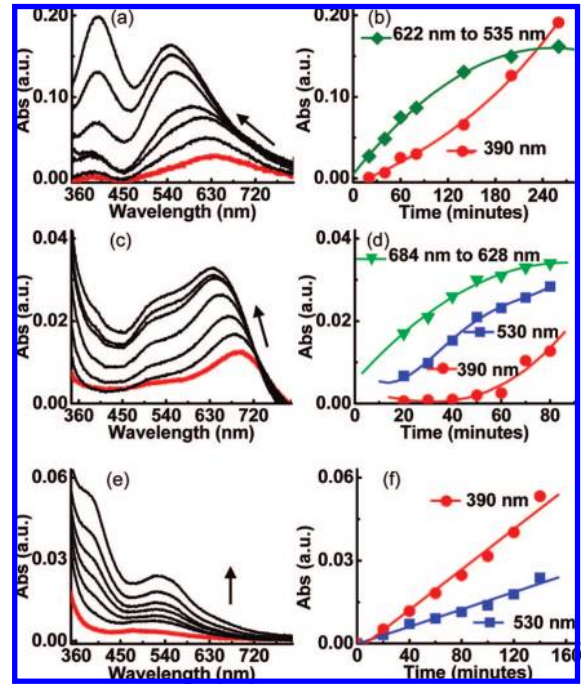

Figure 2. (a, c, e) Time evolution of the UV−vis−NIR spectra of ABA polymerization processes in 0.5 M H_2SO_4 at 16 °C: (a) 10 mM ABA with an SWNT/ABA ratio of 1:200; (c) 2.5 mM ABA with an SWNT/ABA ratio of 1:50; (e) 50 mM ABA without ssDNA−SWNTs. (b, d, f) Time dependence of the growth of the intensities of the peaks shown in (a), (c), and (e), respectively. The peak intensities for the peaks were obtained using a peak-fitting program with nonbaseline and Gaussian peak-fit components (Grams/32 AI). The peak-fitting treatment of a typical UV−vis spectrum (the one at 80 min in panel c) is shown in Figure S1 in the Supporting Information.

polymerization time studied (Figure 2e,f). It should be noted that we used 50 mM instead of 10 mM ABA for studying the neat ABA polymerization because of its extremely low rate.

As the polymerization progressed, the peak at 622 nm gradually shifted to 570 nm and then stabilized at 530 nm, the same position as the polymer peak that appeared for the ABA polymerization in the absence of ssDNA−SWNTs (Figure 1a, blue curve, and Figure 2e). Interestingly, the ABA oligomer peak at 390 nm grew slowly in the beginning and then much more rapidly as the 622 nm peak gradually blue-shifted to 530 nm (Figure 2a,b).

From these results, we now obtain the following scenario: during polymerization in the presence of ssDNA−SWNTs, PABA is first polymerized along the CNTs, producing the "real" PABA/SWNT composite (where "real" refers to the composite whose properties are different from those of both SWNTs and neat PABA.) The PABA in the real composite, which is at the interface between the carbon nanotubes and the bulk polymer, has longer conjugation lengths and exists mainly in the stable emeraldine state.[29] It is worthy of mention that this interfacial layer can extend far beyond the regions where the PABA intimately contacts the carbon nanotubes.[11,32] This can be explained by proposed models for growth of polyaniline via chemical oxidative polymerization.[33,34] There are two possible types of nucleation sites: those in the bulk solution and those

(30) Deore, B. A.; Hachey, S.; Freund, M. S. *Chem. Mater.* **2004**, *16*, 1427–1432.
(31) Fu, Y.; Elsenbaumer, R. L. *Chem. Mater.* **1994**, *6*, 671–677.
(32) Winey, K. I.; Kashiwagi, T.; Mu, M. *MRS Bull.* **2007**, *32*, 348–353.
(33) Chiou, N.-R.; Lu, C.; Guan, J.; Lee, J. L.; Epstein, A. J. *Nat. Nanotechnol.* **2007**, *2*, 354–357.
(34) Liang, L.; Liu, J.; Windisch, C. E.; Wxarhos, G. J.; Lin, Y. *Angew. Chem., Int. Ed.* **2002**, *41*, 3665–3668.

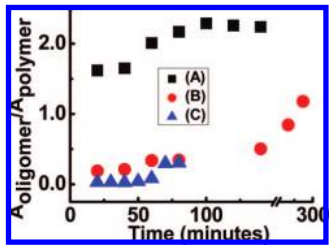

Figure 3. Ratios of the absorbance intensities of the ABA oligomer peak at 390 nm and the peak(s) for the PABA polymers (both free and in the real composite) as functions of time for polymerization of (A) neat 50 mM ABA (black squares), (B) 10 mM ABA with an SWNT/ABA ratio of 1:200 (red circles), and (C) 2.5 mM ABA with an SWNT/ABA ratio of 1:50 (blue triangles). The intensities of the oligomer and polymer peaks were obtained using the peak-fitting procedure described in Figure 2.

on the carbon nanotubes. These two kinds of sites compete with each other. In the beginning, PABA nucleation is faster on the carbon nanotubes, and therefore, the initial nucleation leads to the formation of PABA with longer conjugation lengths and better-ordered molecular structures as a result of the templating effect of the carbon nanotubes. The initially formed PABA layer may minimize the interfacial energy barrier for subsequent growth of PABA around the carbon nanotubes and have secondary impacts on both the polymerization rate and the structures of the subsequently grown PABA. As more PABA layers grow, this influence becomes diminished, and more "free" PABA (i.e., PABA that is not impacted by the presence of CNTs) and short ABA oligomers start to form. At the same time, nucleation sites in the bulk solution start to form and dominate the PABA growth.

To further support this conclusion, we increased the SWNT/ABA ratio to 1:50 by decreasing the ABA monomer concentration to 2.5 mM. The combined absorption peak for PABA in the real composite and free PABA (Figure 2a,b) split into two peaks; we were able to simultaneously see these two different polymer structures (Figure 2c,d) during the polymerization process, which provided strong support to our hypothesis described above.

In the 1:50 polymerization, λ_{max} for the real composite was 684 nm, which was larger than that for the 1:200 case. In the first 10 min, most of the product was the real composite, as shown in the bottom (red) spectrum in Figure 2c. The intensity of the composite peak rapidly increased during the first 40 min, after which the intensity increase became slower. Meanwhile, the peak gradually blue-shifted to a λ_{max} of 628 nm. In contrast, the free PABA peak at 530 nm evolved slowly at the beginning and more rapidly at later times. Remarkably, the intensity of the absorption at 390 nm did not grow in the first 20 min, indicating that almost no ABA oligomers were produced during this time period.

Figure 3 summarizes the time evolutions of the ratio of the intensities of the ABA oligomer peak and the peak(s) for the PABA polymers (both free and in the real composite) as the various polymerizations progressed. It is very obvious that without ssDNA−SWNTs, a larger amount of ABA oligomers relative to the polymers was produced. In the presence of ssDNA−SWNTs, the formation of ABA oligomers was largely eliminated at the beginning of the polymerization. With a greater loading of ssDNA−SWNTs in the polymerization solution, fewer ABA oligomers were produced. It is worth mentioning that at longer polymerization times, probably after the formed PABA covered the surface of the SWNTs, ABA oligomers started to grow more rapidly.

Conducting polymers with longer conjugation lengths are expected to have better conductivities.[35,36] The presence of oligomers in a conducting polymer significantly decrease its conductivity and stability. The capability of ssDNA−SWNTs to simultaneously eliminate the formation of short oligomers and facilitate the production of polymers with longer conjugation lengths can be exploited to produce conducting-polymer composite materials with much-enhanced electronic performance. Understanding the growth pattern during the polymerization process can guide us in optimizing the conditions in order to produce highly conductive composite materials.

Catalytic Effect of ssDNA−SWNTs. As discussed earlier, the polymerization efficiency was greatly increased by the addition of 0.5 wt % ssDNA−SWNTs to the polymerization solution (Figure 2a,b). When the loading of ssDNA−SWNTs in the solution was increased to 2% (Figure 2c,d), the growth rate of the peak at 684 nm was 1.1×10^{-3} min^{-1} during the first 10 min of polymerization (Figure 2c,d). Apparently, the polymerization process was 11 times faster than that of neat ABA polymerization (Figure 2e,f) even though the concentration of ABA was 20 times lower.

In our previous work,[37] we have demonstrated that ssDNA−SWNTs can be used as molecular templates to fabricate PABA composite nanowires because of their ability to pre-emulsify or self-assemble[38] the ABA monomers along the ssDNA−SWNTs before polymerization. We also found that the rate of electrochemical polymerization of ABA monomers was greatly increased with ssDNA−SWNTs on the electrode surface. However, at that stage of the study, we were not sure whether the ssDNA−SWNTs catalyzed the polymerization, since preconcentration of the monomers along the ssDNA−SWNTs could produce similar effects. In the present work, we observed that the absorption peak for the real composite appeared first during the polymerization, suggesting that PABA was initially polymerized along the CNTs. To determine whether the observed fast polymerization was due to a preconcentration effect or a catalytic effect of the ssDNA−SWNTs during ABA oxidative polymerization, we roughly estimated the rate constant for ABA polymerization in the presence or absence of ssDNA−SWNTs using a simplified model.

The kinetics of chemical polymerization of aniline and aniline derivatives has been studied in the presence or absence of solid substrates.[39] If the substrates could catalytically oxidize aniline, the polymerization rate constant would be substantially increased by an amount that would depend on both the catalytic nature of the substrates toward aniline oxidation and the quantity of the substrate in the polymerization solution.

Two models have been used to describe the kinetics of chemical polymerization of aniline and aniline derivatives. In most cases, the produced polymers have been found to precipitate during polymerization, thereby increasing the polymerization rate. Tzou and Gregory[39] proposed an autoacceleration reaction mechanism involving surface effects of the formed polymer, as in the self-acceleration reaction observed during electrochemical polymerization of aniline.[40] However,

(35) Lee, K.; Cho, S.; Park, S. H.; Heeger, A. J.; Lee, C.-W.; Lee, S.-H. *Nature* **2006**, *441*, 65–68.
(36) MacDiarmid, A. G. *Angew. Chem., Int. Ed.* **2001**, *40*, 2581–2590.
(37) Ma, Y. F.; Ali, R. K.; Dodoo, A. S.; He, H. X. *J. Phys. Chem. B* **2006**, *110*, 16359–16365.
(38) Zhou, W.; Fischer, J. E.; Heiney, P. A.; Fan, H.; Davis, V. A.; Pasquali, M.; Smalley, R. E. *Phys. Rev. B* **2005**, *72*, 045440.
(39) Tzou, K.; Gregory, R. V. *Synth. Met.* **1992**, *47*, 267–277.
(40) Wei, Y.; Sun, Y.; Tang, X. *J. Phys. Chem.* **1989**, *93*, 4878.

Table 1. Comparison of Polymerization Rate Constants (k) for in Situ Polymerization of ABA for 10 min in the Presence of Different Substrates

	neat	in situ ssDNA−SWNTs		seed method	ssDNA only
ABA concentration (mM)	50	10	2.5	50	50
substrate concentration	−	1:200 (w/w)	1:50 (w/w)	1:50 (w/w)	0.51 μM
k (M^{-2} min^{-1})[a]	2.9×10^{-3}	4.1	13	1.1×10^{-3}	8.7×10^{-3}
enhancement factor[b]	1	~1,400	~4,500	~0.4	3

[a] k values for in situ ssDNA−SWNTs are for production of the real composite; other k values are for production of the free PABA polymer. [b] Defined as the ratio of the k value for ABA polymerization in the presence of the substrate to that for neat ABA polymerization.

if the produced polymers were soluble, then the autoacceleration effect of the formed polymer would be negligible. Sivakumar et al.[41,42] proposed an empirical kinetic equation to describe this polymerization process. In the current study, no PABA was found to precipitate during the polymerization times used. Therefore, we applied a simplified model (eq 1) to estimate the rate constants under the three sets of polymerization conditions described above:

$$-\frac{d[ABA]}{dt} = k[ABA]^2[APS] \quad (1)$$

where [ABA] and [APS] are the concentrations of ABA and APS at polymerization time t and k is the rate constant for the formation of PABA. We calculated the rate constant for ABA polymerization in the first 10 min (Table 1). For neat ABA polymerization, the calculated value of k was 2.9×10^{-3} M^{-2} min^{-1}. For an SWNT/ABA ratio of 1:200, the k value increased to 4.1 M^{-2} min^{-1}, which is 1,400 times higher than that for neat ABA polymerization. When the SWNT/ABA ratio was increased to 1:50, the k value for formation of PABA in the real composite increased to 13 M^{-2} min^{-1}, which is 4,500 times higher than that for neat ABA polymerization. These results show that in the presence of ssDNA−SWNTs, the k value increased dramatically by an amount that depended on the ratio of the concentrations of ABA monomers and ssDNA−SWNTs. The large increase in k unambiguously suggests that ssDNA−SWNTs had a significant catalytic effect on the oxidative polymerization of ABA.

Inability of Fe_2O_3 To Enhance the Rate of ABA Polymerization. We used atomic absorption spectroscopy to determine the concentration of iron oxide residues in the ssDNA−SWNT solution. We found that the iron concentration was 1.7 ppm after the ssDNA−SWNT solution was dialyzed against deionized water for 4 h. To examine if the catalytic behavior revealed here was due to the Fe_2O_3 residues, we added 86 mg of Fe_2O_3 particles to the ABA polymerization solution, giving an iron concentration of 10 ppm. The results showed that the addition of Fe_2O_3 to the solution did not speed up the polymerization. It is known that Fe^{3+} can also oxidize aniline and initialize aniline polymerization.[43] Since the ABA polymerization was performed in 0.5 M H_2SO_4, Fe^{3+} must have existed in the polymerization solution. A control experiment was also performed in which 10 ppm Fe^{3+} was added to the ABA polymerization solution (Figure S2 in the Supporting Information]. The results did not indicate that Fe^{3+} had any catalytic effect on the polymerization of ABA. Therefore, we conclude that the catalytic effect we observed in this work was not due to Fe_2O_3 residues in the ssDNA−SWNTs. Instead, it must be due to the electronic structure of the CNTs and their interactions with the ABA monomers.

Electronic Study of the Interactions between ABA Monomers and ssDNA−SWNTs. To understand the origin of the catalytic effect of the ssDNA−SWNTs during the in situ polymerization process, we studied the interactions between ssDNA-functionalized CNTs and ABA monomers using UV−vis−NIR electronic absorption spectroscopy. This is an extremely powerful tool for studying the electronic structures of carbon nanotubes that has been used to study band-gap-selective protonation of SWNTs[44] and electron-transfer reactions of SWNTs with small inorganic redox reagents[45] and organic acceptor molecules.[14] It was observed that electron transfer from CNTs could diminish their absorption intensities. The UV−vis−NIR bleaching sometimes accompanied red-shifts of the absorption peaks. It has been reported that ABA is electron-deficient because of the sp^2 hybridization of the boron.[46] Therefore, it is very possible that a charge-transfer complex may form upon addition of ABA monomers to the ssDNA-SWNT solution. The interactions between the ABA monomers may change the charge density of the CNTs, which would induce UV−vis−NIR bleaching or shifting of peak positions for certain nanotubes. It has been reported that dissolved O_2 can oxidize CNTs in acidic solutions, causing UV bleaching and fluorescence quenching in the near-IR region of the E_{11} transitions.[44,47] Since polymerization of ABA requires acidic conditions, the electronic study using UV−vis−NIR was performed with bubbling of N_2 in order to minimize SWNT oxidation by O_2, as in the in situ polymerization studies.

Figure 4 shows UV−vis−NIR spectra of the ssDNA−SWNTs before and after addition of ABA monomers under N_2. The E_{11} and E_{22} peaks were respectively assigned to the first and second van Hove interband transitions in the density of states of semiconducting SWNTs.[48,49] We found that even under N_2, the E_{11} and E_{22} peaks were partially bleached when the pH of the ssDNA−SWNT solution was adjusted from 7.4 (Figure 4a, green curve) to 1 (Figure 4a, blue curve). This result is consistent with previous reports indicating that the nanotubes were partially oxidized by dissolved O_2,[44,47] since complete removal of O_2 required UV illumination.[14,47] After addition of ABA to the solution at pH 1 (Figure 4a, red curve), the E_{11} peaks for the first van Hove transitions (1000−1300 nm) were further

(41) Sivakumar, C.; Gopalan, A.; Vasudevan, T.; Wen, T.-C. *Synth. Met.* **2002**, *126*, 123–135.
(42) Sivakumar, C.; Gopalan, A.; Vasudevan, T.; Wen, T.-C. *Ind. Eng. Chem. Res.* **2001**, *40*, 40–51.
(43) Sun, Z. Y.; Geng, Y.; Li, J.; Wang, X.; Jing, X.; Wang, F. *J. Appl. Polym. Sci.* **1999**, *72*, 1077–1084.
(44) Strano, M. S. *J. Phys. Chem. B* **2003**, *107*, 6979–6985.
(45) Zheng, M.; Diner, B. A. *J. Am. Chem. Soc.* **2004**, *126*, 15490–15494.
(46) Shoji, E.; Freund, M. S. *J. Am. Chem. Soc.* **2002**, *124*, 12486–12493.
(47) Dukovic, G.; White, B. E.; Zhou, Z. Y.; Wang, F.; Jockusch, S.; Steigerwald, M. L.; Heinz, T. F.; Friesner, R. A.; Turro, N. J.; Brus, L. E. *J. Am. Chem. Soc.* **2004**, *126*, 15269–15276.
(48) Itkis, M. E.; Niyogi, S.; Meng, M. E.; Hamon, M. A.; Hu, H.; Haddon, R. C. *Nano Lett.* **2002**, *2*, 155–159.
(49) Chiang, I. W.; Brinson, B. E.; Huang, A. Y.; Willis, P. A.; Bronikowski, M. J.; Margrave, J. L.; Smalley, R. E.; Hauge, R. H. *J. Phys. Chem. B* **2001**, *105*, 8297–8301.

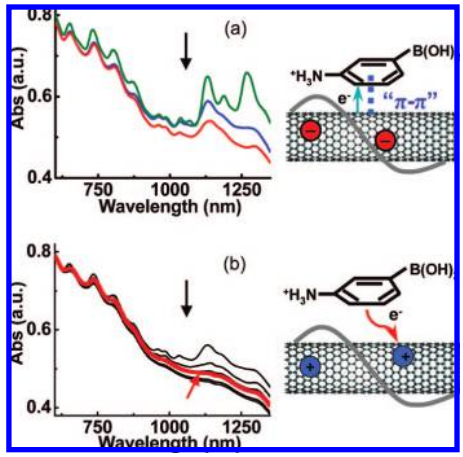

Figure 4. (a) UV−vis−NIR spectra of ssDNA−SWNTs under N_2 (green curve) at pH 7.4 and (blue curve) before and (red curve) after addition of ABA monomers at pH 1. (b) UV−vis−NIR absorption spectra recorded under N_2 at pH 1 (black curves) during oxidation of ssDNA−SWNTs by addition of 1 μL aliquots of 37.5 mM APS every 20 min to a total of 10 μL and (red curve) immediately after addition of 50 μL of 50 mM ABA.

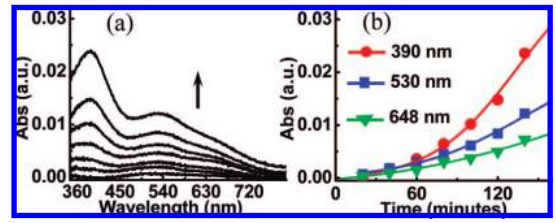

Figure 5. (a) UV−vis−NIR spectra monitoring the progress of polymerization using the seed approach at 16 °C in 0.5 M H_2SO_4 with 50 mM ABA and an SWNT/ABA ratio of 1:50. (b) Increases in the peak intensities at (red curve) 390 nm, (blue curve) 530 nm, and (green curve) 648 nm as the polymerization progressed. Peak intensities were obtained using the peak-fitting procedure described in Figure 2 caption.

bleached, as indicated by the black arrow. This result may suggest that complexes of ABA with SWNTs were formed. In these complexes, electrons would be partially transferred from the SWNTs to ABA, resulting in higher electron densities for complexed ABA than for free ABA monomers.

An oxidative polymerization mechanism for the polymerization of aniline and aniline derivatives has been proposed.[39] The first step is production of aniline radical cations by oxidation. It has been reported that ABA monomers are more difficult to oxidize than native aniline because of the electron-withdrawing boronic acid functional group.[46,50] Addition of F^- to the polymerization solution yields a tetrahedral anionic complex[46] in which the electron-withdrawing nature associated with the vacant p orbital on the boron atom is eliminated.[46,50] This complex acts as the precursor for ABA polymerization, where a much lower potential is needed for electrochemical polymerization. This is the principle of fluoride-catalyzed polymerization of PABA under acidic conditions.[46,50]

We hypothesize that in the present case, the SWNT−ABA complexes acted as the polymerization precursors. Because of the electron-rich nature of the ssDNA−SWNTs, the ABA monomers had higher electron densities, which greatly facilitated the polymerization. If this assumption is true, electron-deficient SWNTs may slow the polymerization process. To explore this possibility, we performed the experiments described below.

Seed Approach. It was reported that addition of APS into CNT solutions before addition of the monomers could cause oxidation of the nanotubes and that the oxidized CNTs could oxidize pyrrole and aniline monomers. This is the basis of the seed process for production of conducting polymer nanowires.[25,26] The authors clearly demonstrated that the morphologies of the polymers produced by this method were greatly influenced by the order in which APS was added to the polymerization solution, but they did not study how the polymerization kinetics was affected. To further understand the dependence of the polymerization kinetics on the electronic structure of the carbon nanotubes, we performed an experiment in which APS was added to the CNT solution to oxidize the nanotubes, producing electron-deficient SWNTs. ABA monomers were then added into the system. Figure 4b shows UV−vis−NIR spectra of the ssDNA−SWNTs at pH 1 before and after addition of APS and following addition of ABA monomers to the oxidized SWNT solution. It is clear that adding APS to the SWNT solution further oxidized the carbon nanotubes, as indicated by the UV−vis−NIR absorption bleaching (Figure 4b, black curves). After introducing ABA into the system (Figure 4b, red curve), we found a slight recovery of the E_{11} absorption peaks (indicated by the red arrow), suggesting that the ABA monomers might partially donate electrons to the oxidized SWNTs and thereby become electron-deficient, as expected.

With this knowledge in mind, we performed another experiment to study the polymerization kinetics involving the electron-deficient SWNTs. In brief, APS was first added to the SWNT solution to oxidize SWNTs. ABA monomers were then added to the oxidized SWNT solution. The concentrations of ABA and ssDNA−SWNTs and the amount of APS added were the same as in Figure 2c,d. However, we did not observe any polymerization even after 6 h under these conditions. We increased the ABA concentration to 50 mM, which is the same as that in Figure 2e,f. The concentration of ssDNA−SWNTs was also increased in order to keep the SWNT/ABA ratio at 1:50 (w/w). The evolution of the UV−vis−NIR spectra is shown in Figure 5. In comparison with the spectra shown in Figure 2c, which were obtained using the same SWNT/ABA ratio of 1:50 but without preoxidation of the SWNTs, the peak for the real composite at 680 nm was not obvious, indicating that a very small amount of PABA with a longer conjugation length was produced using the seed approach. However, the ABA oligomer peak at 390 nm increased more rapidly than the free PABA peak at 530 nm, suggesting that more ABA oligomers were produced. The rate increase at 530 nm was also less than that for the neat ABA polymerization. For example, after 10 min of polymerization, the intensity of the free PABA peak at 530 nm increased at a rate of 3.8×10^{-5} min^{-1}, which is 2.6 times slower than in the case of neat ABA polymerization (1×10^{-4} min^{-1}). This result suggests that the oxidized SWNTs decreased rather than increased the rate of the polymerization process.

The polymerization rate constant k for the seed approach was also calculated using Sivakumar et al.'s empirical kinetic equation (Table 2). The k value for formation of free PABA (530 nm) after 10 min of polymerization was 1.1×10^{-3} M^{-2} min^{-1}, which is a factor of ~1,000 times smaller than that for the polymerization in the presence of the intact ssDNA−SWNTs. The k value for formation of the real composite (648 nm) after 10 min of polymerization was 7.0×10^{-4} M^{-2} min^{-1}, which

(50) Nicolas, M.; Fabre, B.; Marchand, G.; Simonet, J. *Eur. J. Org. Chem.* **2000**, *9*, 1703–1710.

Table 2. Impact of the Electronic Structure of the Carbon Nanotubes on the Kinetics of ABA Polymerization

polymer product	k (M^{-2} min^{-1}) using intact ssDNA−SWNTs	k (M^{-2} min^{-1}) using preoxidized ssDNA−SWNTs (seed method)	k_{intact}/k_{seed}[a]
free polymer	1.2	1.1×10^{-3}	1.1×10^{3}
real composite	13	7.0×10^{-4}	1.9×10^{4}

[a] Defined as the ratio of the k value for ABA polymerization in the presence of intact ssDNA−SWNTs to that in the presence of preoxidized ssDNA−SWNTs.

is 4 orders of magnitude smaller than that for the polymerization in the presence of the intact ssDNA−SWNTs. These huge differences in the values of the polymerization rate constants demonstrate that the electronic structure determines the catalytic ability of the carbon nanotubes.

It is worth emphasizing here that a tiny change in the order in which the chemicals were introduced into the reaction solution affected not only the polymerization rate but also the quality of the product. Figure S3 in the Supporting Information compares the ratio of the absorbances of the ABA oligomer peak and the peaks for the polymers (both free polymers and real composites) obtained using the seed method with the ratio obtained for the in situ polymerization with intact ssDNA−SWNTs. The results show that a much larger amount of ABA oligomer was produced by the seed method than by the polymerization using intact ssDNA−SWNTs, even though the SWNT/ABA ratio was the same (1:50) in the two polymerization solutions. This result demonstrates that the electronic structure of the carbon nanotubes dramatically impacts the quality of the PABA polymer in the composite and therefore the performance of the composite.

Role of ssDNA. It is known that interactions between ABA and DNA may exist, possibly through a dative bond between an NH_2 group in DNA and the boronic acid group in ABA.[51] This interaction could also result in greater electron density in ABA before polymerization. A control experiment using the same concentrations of ABA and ssDNA (which had the same sequence T as that in the ssDNA−SWNTs) was performed in order to study the role of DNA in facilitating the polymerization. The UV−vis−NIR spectra of the polymerization process are shown in Figure S4 in the Supporting Information. The polymerization rate was a factor of 3 greater than that for the polymerization using only ABA monomers (Table 1) but was still much slower than the polymerization rate in the presence of the ssDNA−SWNTs. These results demonstrate that the ABA−DNA interaction was fairly weak. Therefore, the contribution from ssDNA alone in increasing polymerization rate was very small. This result is consistent with our previous study,[37] which showed that ABA monomers mainly interact with the bare graphene sheets existing on the ssDNA−SWNTs.

Summary and Outlook. We found that the ssDNA−SWNTs acted as catalytic molecular templates during in situ polymerization of ABA. Not only was the polymerization rate greatly increased, but the quality of the resulting PABA was also remarkably improved, as demonstrated by the fact that fewer short oligomers were produced and the backbone of the self-doped polyaniline had a longer conjugation length and existed in the more stable and conductive emeraldine state. These advantages could not be obtained by simple mixing of the preformed conducting polymer with the ssDNA−SWNTs. We further demonstrated that the efficacy of ssDNA−SWNTs in promoting the polymerization of a self-doped polyaniline was not due to catalytic residues of iron oxide particles present in the ssDNA−SWNTs; instead, it was due to preconcentration of monomers along the ssDNA−SWNTs and electronic interactions between ABA monomers and ssDNA−SWNTs. Adding the oxidant (APS) to the ssDNA−SWNTs solution before introducing the ABA monomers oxidized the ssDNA−SWNTs. Consequently, the electronic structure of the SWNTs and therefore their interactions with the ABA monomers were changed. Accordingly, the polymerization of ABA was slowed, and the electronic and molecular structures of the PABA in the resulting composite were very different from those in composites fabricated using intact ssDNA−SWNTs. Remarkably, we found that the electrical performance of the SWNT network can be significantly improved by in situ polymerization of a thin layer of PABA on the intact ssDNA−SWNTs.[24] This enhancement could not be achieved by simple postmixing or even by in situ polymerization using preoxidized SWNTs. It has been reported that the conductance of SWNT networks and the percolation threshold were affected by several factors, such as the contact resistance between nanotubes in the network,[52] the spatial distribution of SWNTs in the network,[32] and the level of SWNT doping in the network.[53] Detailed studies of the electronic percolation behavior of the composite networks, the electronic and molecular structures of the PABA, and the distribution of the CNTs in the different composites are essential for understanding the electronic enhancement by the different coating approaches and will be reported in a separate paper.[24]

In addition, boronic acids have recently gained tremendous popularity as substrates and building blocks in organic synthesis and combinatorial chemistry.[54] The remarkable advantage of using PABA as the conducting skin, instead of the parent polyaniline itself, is the existence of the boronic acid groups along the polyaniline backbone, which allows us to introduce different functionalities into the system in order to fit different applications. Lately, it has been demonstrated that PABA can be used as a polyaniline precursor in the fabrication of a wide range of substituted polyanilines.[55,56] Furthermore, the existence of the boronic acid groups also dopes the polyaniline backbone and extends the conductivity and electrochemical activity of the polyaniline to neutral pHs, which is critical for biosensor applications.[29,30,46,57,58] We recently explored these properties for sensitive and selective detection of dopamine in the diagnosis of Parkinson's disease.[37,59,60] The role of the boronic acid groups also includes increasing the water solubilities of the polymer

(51) Recksiedler, C. L.; Deore, B. A.; Freund, M. S. *Langmuir* **2006**, *22*, 2811–2815.
(52) Fuhrer, M. S.; Nygard, J.; Shih, L.; Forero, M.; Yoon, Y.-G.; Mazzoni, M. S. C.; Choi, H. J.; Ihm, J.; Louie, S. G.; Zettl, A.; McEuen, P. L. *Science* **2000**, *288*, 494–497.
(53) Dettlaff-Weglikowska, U.; Skákalová, V.; Graupner, R.; Jhang, S. H.; Kim, B. H.; Lee, H. J.; Ley, L.; Park, Y. W.; Berber, S.; Tománek, D.; Roth, S. *J. Am. Chem. Soc.* **2005**, *127*, 5125–5131.
(54) Hall, D. G., Ed. *Boronic Acids: Preparation and Applications in Organic Synthesis and Medicine*; Wiley-VCH: Weinheim, Germany, 2005.
(55) Rechsiedler, C. L.; Deore, B. A.; Freund, M. S. *Langmuir* **2005**, *21*, 3670–3674.
(56) Shoji, E.; Freund, M. S. *Langmuir* **2001**, *17*, 7183–7185.
(57) Deore, B. A.; Yu, I.; Freund, M. S. *J. Am. Chem. Soc.* **2004**, *126*, 52–53.
(58) Deore, B. A.; Yu, I.; Aguiar, P. M.; Recksiedler, C.; Kroeker, S.; Freund, M. S. *Chem. Mater.* **2005**, *17*, 3803–3805.
(59) Ali, S. R.; Ma, Y. F.; Parajuli, R. R.; Balogan, Y.; Lai, W. Y.-C.; He, H. X. *Anal. Chem.* **2007**, *79*, 2583–2587.

and the composite, which are very different from that of the parent polyaniline.[29] This remarkable property could allow us to fabricate large-area composite films using the same room-temperature coating techniques as were used to fabricate CNT networks,[20,24,61–65] as described in detail in the subsequent paper.[24] In summary, the functionality of the boronic acid functional group of ABA and the highly improved electronic performance of the PABA/SWNT composite networks may stimulate development of a broad range of applications, especially in high-performance flexible electronics and sensors.

(60) Ali, S. K.; Parajuli, R. R.; Ma, Y. F.; Balogan, Y.; Lai, W. Y.-C.; He, H. X. *J. Phys. Chem. B* **2007**, *111*, 12275–12281.
(61) Kaempgena, M.; Duesbergb, G. S.; Rotha, S. *Appl. Surf. Sci.* **2005**, *252*, 425.
(62) Artukovic, E.; Kaempgen, M.; Hecht, D. S.; Roth, S.; Gruner, G. *Nano Lett.* **2005**, *5*, 757–760.
(63) Kordás, K.; Mustonen, T.; Tóth, G.; Jantunen, H.; Soldano, C.; Talapatra, S.; Kar, S.; Vajtai, R.; Ayayan, P. *Small* **2006**, *2*, 1021–1025.
(64) Simmons, T. J.; Hashim, D.; Vajtai, R.; Ajayan, P. M. *J. Am. Chem. Soc.* **2007**, *129*, 10088–10089.
(65) Zhang, D.; Ryu, K.; Liu, X.; Polikarpov, E.; Ly, J.; Tompson, M. E.; Zhou, C. *Nano Lett.* **2006**, *6*, 1880–1886.

Acknowledgment. The American Chemical Society Petroleum Research Fund and the National Science Foundation under CHE-0750201 are acknowledged for partial support of this study. A.S. thanks the Minority Biomedical Research Support Program, and S.R.A. acknowledges an Undergraduate Research Fellowship from Rutgers University.

Supporting Information Available: Figures S1−S4 mentioned in the text. This material is available free of charge via the Internet at http://pubs.acs.org.

JA7112189